Upgrading and Relocation of the Campbell Meteorological Station in the Széchenyi István Geophysical Observatory

Karolina Szabóné André[1*], Csaba Molnár[1], Tibor Molnár[1], Dániel Piri[1], Csongor Szabó[1], Judit Szendrői[1], Viktor Wesztergom and József Bór[1]

[1]HUN-REN Institute of Earth Physics and Space Science, Sopron, Hungary

Abstract

The main meteorological station at the Széchenyi István Geophysical Observatory equipped mostly with Campbell Scientific meteorological instruments has undergone a major change in recent years. Data download from the data logger has been automated by a mini-PC, new instruments have been added (ceilometer, visibility and present weather sensor, barometer) and the station has been moved to a new location. Now it better complements the atmospheric measurements in the observatory, for example by facilitating the determination of the so-called fair-weather conditions for the evaluation of atmospheric potential gradient measurements. Additionally, a cooperation with the Hungarian Meteorological Service (HMS) has been established, in the framework of which meteorological data are transmitted from the observatory to the HMS. Plots of the station data, updated every 10 minutes, are available on the observatory's website.

Keywords: meteorological measurements, weather, ceilometer, visibility sensor.

Brief History of the Station Before 2021

A meteorological station was installed in the Széchenyi István Geophysical Observatory (NCK) near Nagycenk, Hungary, at the end of 1997 to support other measurements such as the atmospheric electric potential gradient (PG) measurements. Temperature, relative humidity, wind speed, wind direction, global solar radiation, and precipitation data was logged in 10-minute temporal resolution using a Campbell CR10X datalogger (Figs. 1 and 2, Table I). The station

*Corresponding author: Karolina Szabóné André (szabone.a.karolina@epss.hu)
Citation: K. Szabóné André, Cs. Molnár, T. Molnár, D. Piri, Cs. Szabó, J. Szendrői, V. Wesztergom and J. Bór (2025): Upgrading and relocation of the Campbell meteorological station in the Széchenyi István Geophysical Observatory. *Geophysical Observatory Reports, 2023–2024*, 22–40. https://doi.org/10.55855/gor2024.2

was located near the so-called ionosonde house in a sheltered place surrounded by trees (Fig. 3a).

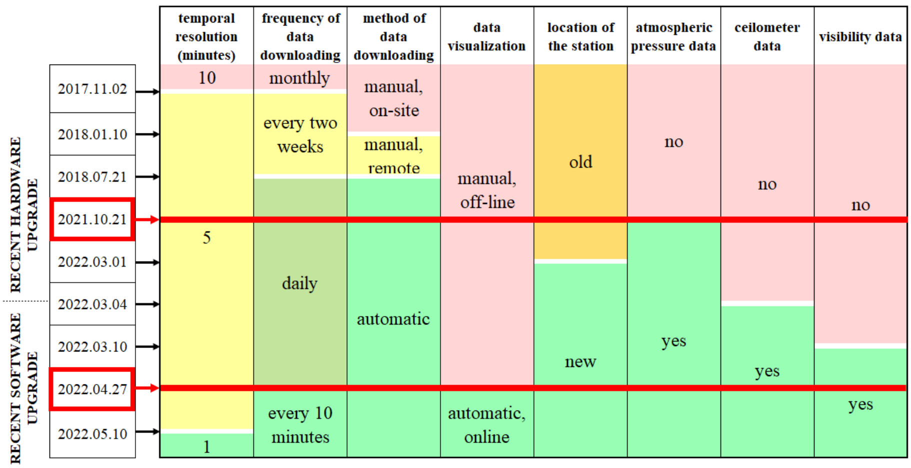

Fig. 1. Evolution of the Campbell meteorological station between 2017 and 2022. The upper red line indicates the recent hardware upgrade which started on 21th October 2021 when the newly purchased barometer was installed. The second red line indicates the recent software upgrade (27th April 2022), the implementation of programs to process data from the new instruments and display all data every 10 minutes.

The first data series of the station was published in the Geophysical Observatory Reports: 1999–2001 (2003). The measurements were suspended in 2012 and were resumed only at the end of August 2017. Data was manually backed up from the data logger quasi monthly using a laptop. A mini-PC was installed in 2018. This enabled automatic daily backup of data from the data logger.

When PG data is evaluated, it is essential to know whether there were fair weather conditions at the measurement site (Harrison and Nicoll, 2018). It is important to have data about the cloud cover, hydrometeors, and wind speed measured at 10 m above ground level. The first two parameters can be determined using a ceilometer and a visibility and present weather sensor. Besides, a meteorological station is incomplete without a barometer measuring the atmospheric pressure. The need to purchase these instruments has therefore arisen and has been fulfilled in the framework of the INFRA tender of the Eötvös Loránd Research Network (ELKH) in 2021.

Fig. 2. The Campbell meteorological station, surrounded by trees in its original location.

Relocation of the Station and Installation of the New Instruments

The station was moved from its original location to a more open place near the PG measurements (Figs. 3 and 4) on 1st March 2022. The newly purchased barometer was placed into the box of the datalogger on the main tower, and it is operating since 21st October 2021. The ceilometer as well as the visibility and present weather sensor were installed during the relocation of the station. Some details about the instruments can be found in Table I.

LIDAR Ceilometer

A SkyVUE PRO light detecting and ranging (LIDAR) ceilometer was purchased from the Campbell Scientific Ltd. The instrument uses short pulses of near infra-red light ($\lambda = 915 \pm 5$ nm with 10 kHz pulse frequency) to detect cloud layers. The emitted short pulses are scattered back from aerosol particles of the atmospheric column above the instrument. The measured (raw) back-scattered data is calibrated and range corrected by the instrument to obtain the so-called two-way attenuated backscatter profile (hereinafter referred to as attenuated

Table I. Some details about the instruments in operation at NCK.
*elevation of the barometer is above mean sea level.

Instrument	Location	Elevation above ground level	Link
Väisälä humidity and temperature probe	main tower (loc. 1 on Fig. 3)	2.0 m	HMP35D manual
Väisälä barometer	main tower (loc. 1 on Fig. 3)	154.66 m*	PTB110 manual
Young wind monitor	main tower (loc. 1 on Fig. 3)	2.4 m	05103-LC
Skye Instruments Pyranometer	main tower (loc. 1 on Fig. 3)	2.0 m	SP1110
Tipping bucket rain gauge	loc. 4 on Fig. 3	1.3 m	ARG100 brochure manual
Visibility and present weather sensor	loc. 2 on Fig. 3	1.5 m	CS125
HygroVUE5 humidity and temperature probe	loc. 2 on Fig. 3	1.5 m	HygroVUE5 manual
LIDAR ceilometer	loc. 3 on Fig. 3		SkyVUE PRO manual

backscatter profile; SkyVUE PRO manual, 2022, Appendix A). This variable is reported by the instrument besides other cloud-related data. The height of the scattering aerosols can be obtained from the time difference between the emitted and back-scattered signal. The strength of the back-scattered light varies with height and this data allows identification of cloud bases. If there is significant scattering but the cloud base cannot be defined, then the vertical visibility can be calculated. The maximum reporting range of the SkyVUE PRO LIDAR is 10 km, and the reporting resolution is 5 m.

Visibility and Present Weather Sensor

A CS125 Visibility and Present Weather sensor (hereinafter referred to as CS125) was also purchased from Campbell Scientific Ltd. This instrument uses infra-red light ($\lambda = 850 \pm 35$ nm with 1 kHz light pulse rate) to determine visibility and to identify hydrometeors (e.g., mist, fog, rain, etc.). The state of

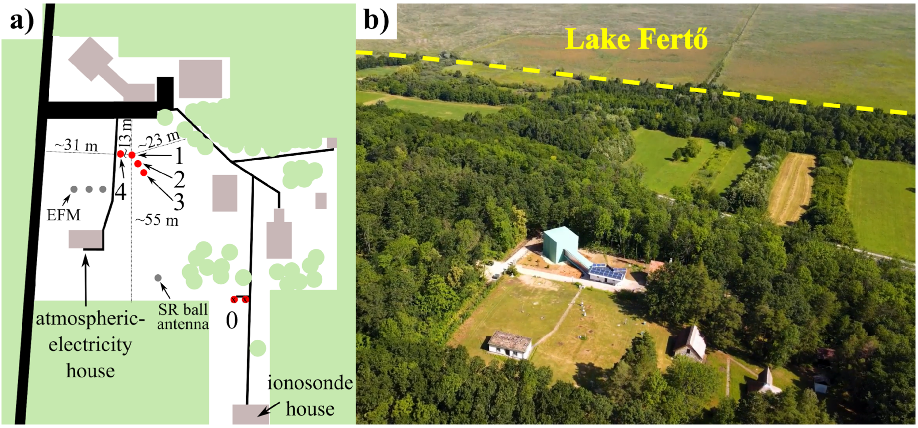

Fig. 3. a) Location of the Campbell meteorological station in the observatory: location before (0) and after 1st March 2022 (1: main tower, 2: visibility and present weather sensor (CS125), 3: ceilometer (LIDAR), and 4: tipping bucket rain gauge). Green area and circles indicate forest and individual trees, respectively. The Boltek Electric Field Monitor (EFM) and the two radioactive instruments measuring the atmospheric electric potential gradient are marked by three grey dots. **b)** A photo of the surroundings of the NCK observatory at the end of June 2022. The shore of Lake Fertő is marked by a yellow dashed line. Source of original photo: website of the EPSS (EPSS news, 2022).

present weather can be reported in the form of e.g., SYNOP and METAR code (WMO, 2019; Milrad, 2017; Wikipedia, 2022). Besides, the CS125 can report precipitation intensity (mm/h). A HygroVUE5 temperature and relative humidity sensor is connected to the CS125 to make more precise discrimination between liquid and frozen precipitation. The measuring range of the CS125 is from 5 m to 75 km (visibility).

Collaboration with the Hungarian Meteorological Service

For better utilization of the new instruments, a cooperation has been established between the HUN-REN Institute of Earth Physics and Space Science (EPSS) and the Hungarian Meteorological Service (HMS). Ceilometers as well as visibility and present weather sensors provide very useful information to support e.g., aviation services. In Hungary, nine ceilometers are in operation in the Tiszántúl Region, one in Budapest and other two in the Transdanubia (Siófok and Pécs) (Fig. 5), and data from theses sensors are collected in the E-profile database (E-profile, 2022). In Little Hungarian Plain (northern part of Transdanubia), there has been no such measurement so far, therefore our new instrument at Fertőboz, near Sopron can fill this gap. Registration to the E-profile database and preparation of data transmission to the E-profile database was in progress at the time of writing this paper. The transmission of ceilometer data as well

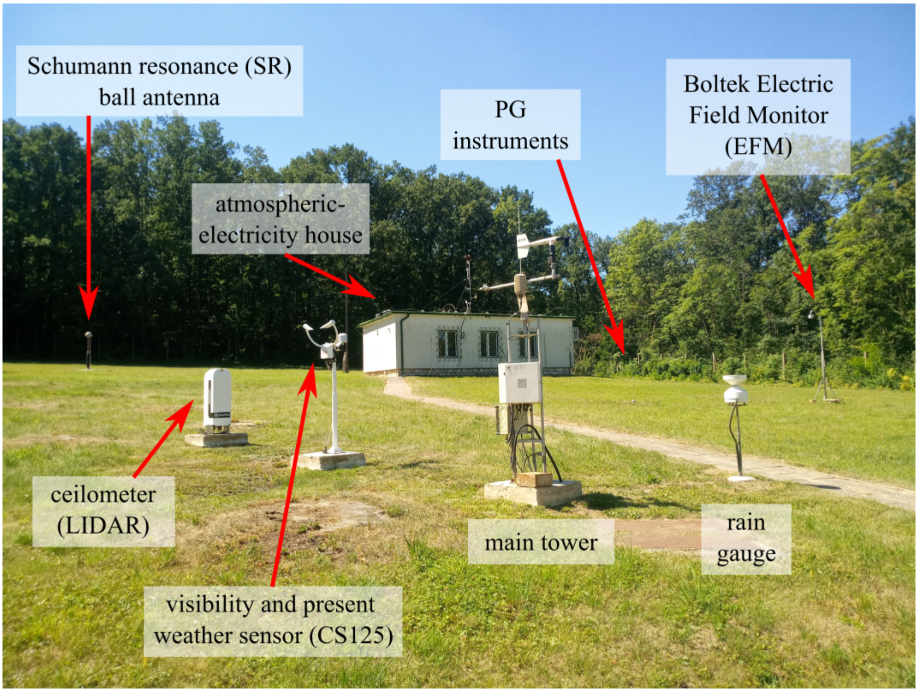

Fig. 4. The Campbell meteorological station with the new instruments at its new location since 1st March 2022.

as visibility and present weather sensor data to the HMS is already operational. Additionally, all data collected with the CR10X data logger enriches the HMS meteorological database.

Data Processing System

A MeLE StarCloud PCG02 Plus stick PC (mini-PC) is placed in the box of the CR10X datalogger in the main tower of the meteorological station. This mini-PC runs a Windows 10 Home operating system and it performs the data obtaining, processing, forwarding, archiving, and plotting tasks. The CR10X datalogger, the LIDAR and the CS125 are connected to the mini-PC via RS232-USB cables. The LIDARs adapter is connected directly through one of the two USB ports of the mini-PC. The other two devices are connected through a USB-hub. Note: an experimental atmospheric pressure measurement based on a simple sensor (BOSCH BME280) is also installed on the main tower. This instrument is also connected to the mini-PC through the USB-hub.

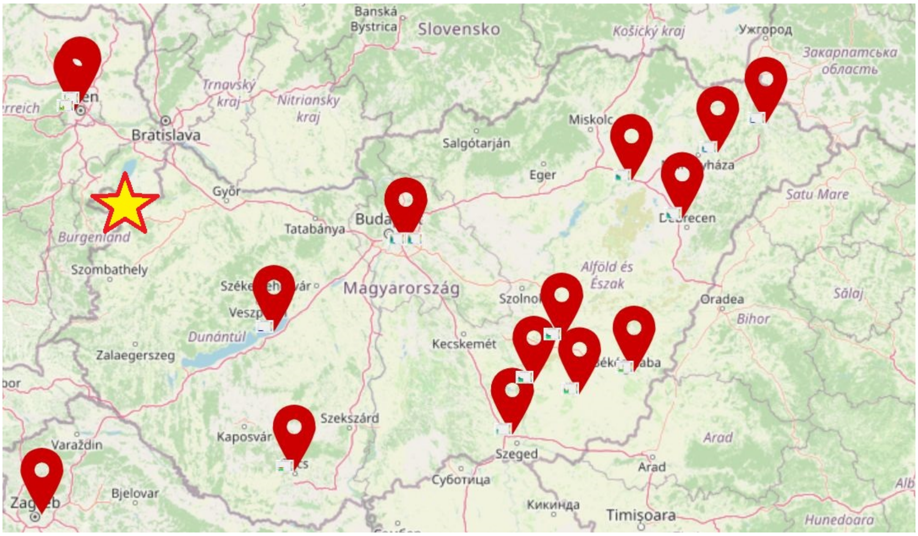

Fig. 5. Location of the LIDAR stations of the E-profile network in Hungary and its surroundings. The location of the new LIDAR (Fertőboz) is marked with a star. Source of the map: E-profile (2022), edited by the Authors.

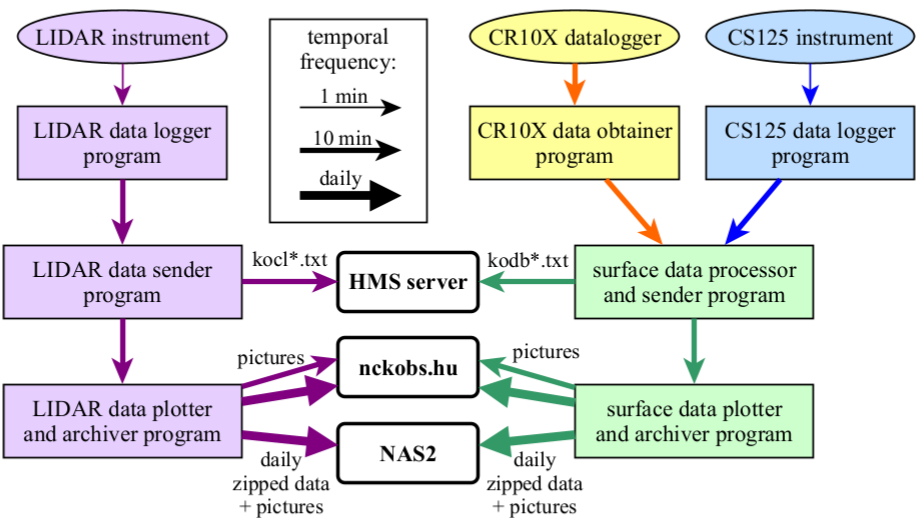

Fig. 6. Data flow of the Campbell measuring system. HMS server is the data-receiving gateway of the Hungarian Meteorological Service (HMS), NAS2 is the network-attached storage service of the HUN-REN Institute of Earth Physics and Space Science.

The data processing system is designed to produce data files which can be transmitted to the HMS. Data are divided into two groups. LIDAR telegrams are stored in plain text files (with kocl prefix in the file names), while the data from CR10X and CS125 are merged into a common txt file. These files are called surface data files (with kodb prefix in the file names). Both types of data files contain 10 minutes of data. The name of the data file contains the time point of the last measured data (rounded to the nearest 10 minutes of the hour). The 10-minute data file is transmitted to the HMS FTP server every 10 minutes.

There are seven Python programs which run continuously on the mini-PC (Fig. 6). Three correspond to the LIDAR measurements (purple rectangles in Fig. 6) and the other four programs handle the CR10X, CS125, and surface data (yellow, blue, and green rectangles in Fig. 6). Three programs collect data from the three different instruments. The LIDAR and the CS125 instruments are queried to send data to the mini-PC in every minute (polling mode). Data sent by the instruments are appended to 10-minute data files. Downloading data from the CR10X data logger is only necessary every 10 minutes. Two programs main task is to send data to the HMS server every 10 minutes. LIDAR data files are forwarded as they are received from the instrument but the CR10X and the CS125 data files need to be processed before transferring. The so-called surface data processor and sender program decodes the data, performs the above-mentioned merging, and sends the surface data files to the HMS. Two other programs are used to plot data and transfer pictures to the web server of the observatory (nckobs.hu) every 10 minutes. At the end of the day, these programs archive data files by zipping and sending them to a NAS2 located at the EPSS in Sopron. Daily image files showing the visualized measured data are also transferred to the NAS2 and the nckobs.hu server.

Visualization of Data

The plots produced by the programs described above are published on the Observatory's website in the Data, Meteorological measurements page (Meteorological data at nckobs.hu, 2022). This section is about the information displayed in the figures. The title on all figures contains the first and last time points of the displayed data. It helps following the measurements realtime: the graphs are updated every 10 minutes, and the latest time will also change. If the last time does not change, it indicates that there is a problem with the system (e.g., a measurement stops, or the internet goes down, etc.).

LIDAR Plots

Two figures are produced using LIDAR data. The first one shows the actual data and the second one shows two auxiliary variables for monitoring the state of the instrument.

The first figure consists of three subplots (Fig. 7) showing data which are essential for determining the so-called fair-weather conditions for interpreting PG measurements (Harrison and Nicoll, 2018). One of the fair-weather criteria is no stratus or stratocumulus clouds below 1500 m. Therefore, the 1500 m height above ground level is marked on the first two panels of this figure.

Cloud Base Data The top panel of Fig. 7 shows the instantaneous cloud base data calculated from the individual backscatter profiles. Three cloud layers can be distinguished this way. The latest cloud height values are shown in the legend.

Sky Condition Data The second panel of Fig. 7 shows sky condition data: cloud base and cloud cover. The cloud cover is given in octas, which shows how many eighths of the full spherical angle of the sky are covered by clouds. These values are calculated from backscatter data of the latest half an hour with cloud data in the previous 10 minutes given an extra weighting. The sky condition algorithm is described in the manual of the instrument (SkyVUE PRO manual, 2022). Five cloud layers can be distinguished by this method with the SkyVUE PRO LIDAR. If there was detected cloud cover at the time of the last measurement, its data are also shown in the "Latest cloud data" text box in the figure.

Attenuated Backscatter Profile The bottom panel of Fig. 7 shows the attenuated backscatter profile data. The beginning of 31st August 2022 was calm and clear. The green area near the surface is the planetary boundary layer (PBL, Hayden and Pielke, 2016). The PBL is usually thinner during the day than at night. It was about 2000 m during the night and less than 1000 m during the day on 31st August.

Another difference between nighttime and daytime is the strength of the backscattered signal at the upper levels of the observed air column which is greater during daytime. It can be caused by the Sun because its radiation also includes near-infrared light which is used by the LIDAR, and this can increase the overall power of the signal that is detected by the sensor of the LIDAR.

The mostly sunny weather changed during the day. The clouds can be identified on the attenuated backscatter profile as red spots/areas. The persistent precipitation appears as yellowish–reddish formations over large areas after 17 UTC. For technical reasons, the backscattered signal strength is very low above the rain clouds (white area).

Auxiliary Variables The second plot shows two auxiliary variables (Fig. 8). The temperature of the laser (top panel) is usually 40 °C. The LIDAR has a heater so if the weather conditions make necessary it heats the laser up to 80 °C to avoid condensation and freezing of atmospheric moisture on the window.

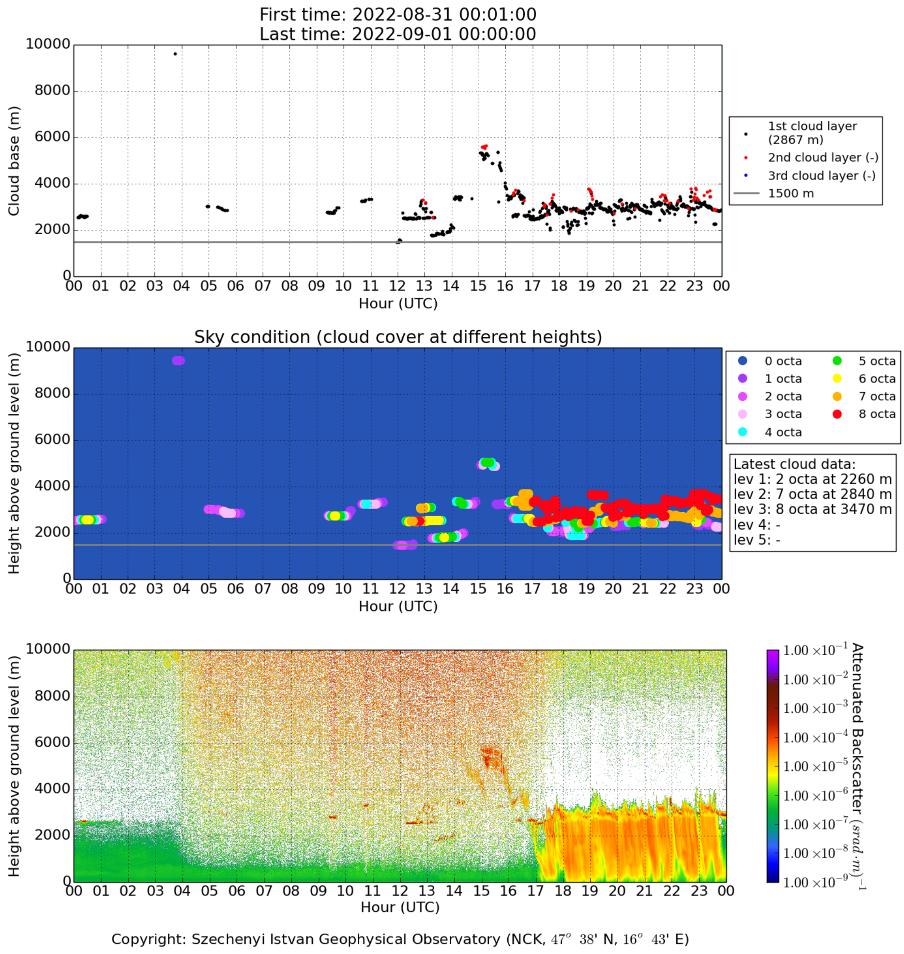

Fig. 7. LIDAR data measured at NCK on 31st August 2022: instantaneous cloud bases (top), sky condition (center) and attenuated backscatter profile (bottom).

The second variable is the LIDAR window transmission (bottom panel). The window of the instrument must be cleaned when the transmission drops below 80%.

Present Weather, Visibility, and Precipitation

The CS125 can count the number and measure the speed and size of particles falling in its detecting volume. The HygroVUE5 temperature and relative humidity probe which is connected to the CS125 provides data which is used to improve the discrimination between frozen and liquid precipitation. Based

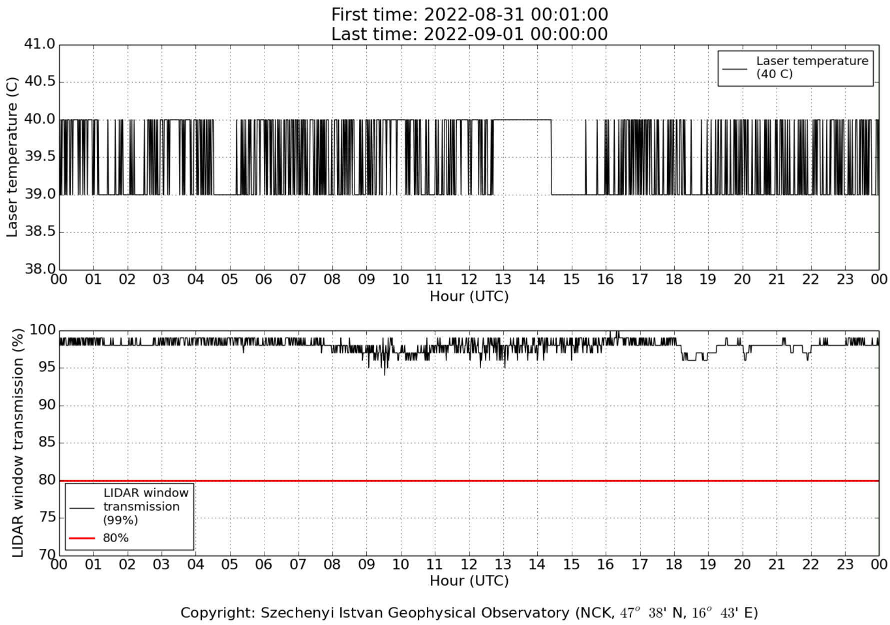

Fig. 8. Auxiliary variables obtained from LIDAR telegram at NCK on 31st August 2022: laser temperature (top) and LIDAR window transmission (bottom).

on these data the sensor can determine the following quantities: *a)* so-called present weather which is a description of the weather phenomena present at the time of observation, *b)* visibility, and *c)* intensity of precipitation.

Present weather data obtained from the CS125 is shown in the upper panel of Fig. 9. The background of the plot is colorful. The different colors correspond to different phenomena which are described in the legend above the plot. Rain is marked in green, snow in blue. Categories that may include solid or liquid precipitation (drizzle, precipitation, shower) are indicated in pink or purple. The thunderstorm category is yellow because of the lightning occurring in thunderstorms. The red line is the present weather reported as SYNOP code (WMO, 2019). Zero value means no significant weather. The precipitation which can be seen in the LIDAR backscatter plot (Fig. 7, bottom panel) is also detected by the CS125. The latest values are shown in the legend in parenthesis: the first value is the SYNOP code (in category /SYNOP code/ format) and the second value, after the comma, is the METAR code. The -DZ means light intensity drizzle. Further description about METAR codes can be found in Milrad (2017) and in the Wikipedia METAR page (Wikipedia, 2022).

The timeseries of visibility is shown in Fig. 9 (second panel). During the rain at the end of 31st August 2022 the visibility was lower than before.

The bottom panel of Fig. 10 shows different quantities related to precipitation: *1)* precipitation intensity determined by the CS125 (orange), *2)* cumulated precipitation calculated from CS125 precipitation intensity with 15% uncertainty also marked (red) and *3)* cumulated precipitation measured by the ARG100 tipping bucket rain gauge and recorded by the CR10X data logger (black). One tilt of the ARG100 means 0.2 mm of precipitation, therefore 0.2 mm is included in the figure as a reference (grey). The precipitation for the day is summed from 00:01 UTC up to 00:00 UTC on the next day to obtain cumulated precipitation. Thus, from the legend of the end-of-day graph, it is possible to see how much precipitation fell that day: 2.6 mm or 3.32 mm fell on 31st August according to the ARG100 and the CS125, respectively. Between 17 and 18 UTC zero tilt was registered by the ARG100 but it was raining according to the CS125. The amount of rain was below 0.2 mm according to the CS125 and it did not saturate the tipping bucket, so the ARG100 did not detect it. This shows that the ARG100 is not strong in measuring small amounts of rain. If the amount of rain is less than 0.2 mm and it does not tip the tipping bucket and the water later evaporates, the precipitation is not recorded. The ARG100 has no built-in heating and is therefore not suitable for real-time measurement of snowfall if the snow can not melt when it falls down (e.g., if the surface temperature of the instrument is under 0 °C). Snow accumulates on the insect net at the top of the funnel and only flows down to the tipping bucket after melting, even days or weeks after the snowfall. It is also possible that the wind blows it off before it melts, or someone removes some or all of the snow from the top of the tipping bucket. This also leads to measurement errors. The ARG100 can produce false measurements even if it is pushed or clogged. However, there could be false precipitation indicated by the CS125 also, if spiders are weaving webs and moving around the sensor, or if light is reflected into the sensor from somewhere, or during cleaning the instrument. In suspicious cases, when the precipitation lasted only a few minutes according to CS125, it is recommended to check the LIDAR backscatter plot, because falling precipitation should be seen on that too. If there is nothing, maybe not even clouds, the precipitation is not real, it should be ignored and the person responsible must look at the instrument. These instruments need to be maintained regularly (e.g., every week). So it can be seen that both instruments have their drawbacks, but together they give a more reliable picture of current rainfall patterns than separately.

Other Surface Plots

Other variables from the so-called surface data files are global solar radiation, temperature, relative humidity (Fig. 10), and atmospheric pressure, wind speed as well as wind direction (Fig. 11). Data from the CS125 data files (HygroVUE5 data) are plotted with red lines in these figures. Other data from the CR10X data logger are plotted with black and blue.

Global solar radiation shows how much sunlight reaches the instrument. Its diurnal cycle is affected by different factors. The effect of trees shadowing the instrument can be seen between 04 and 06 UTC (Fig. 10, upper panel). The global solar radiation increases slowly from 04 to 06 UTC when the Sun rises but the trees shadow the instrument. After 06 UTC global solar radiation starts to increase rapidly when the Sun can shine directly at the instrument above the trees. Due to clouds passing between the Sun and the instrument around 09:30 UTC (see Fig. 7), global solar radiation is reduced. The sky was covered by clouds in the afternoon (lower global solar radiation), but there was a less cloudy period around 15 UTC (see Fig. 7) when the global solar radiation had a local peak on this day.

Both temperature and relative humidity showed a fairly characteristic diurnal cycle on 31st August (Fig. 10, second and bottom panel). The temperature values of the different instruments differ only slightly, while the difference between the two relative humidity data series is larger. The higher the relative humidity, the larger the difference between them. It is because the old Väisälä instrument (black lines) was last calibrated in 2017, but the HygroVUE5 is a factory calibrated, new instrument. This emphasizes the importance of regular calibration at least every few years.

The mean sea level pressure is shown in the top panel of Fig. 11. Wind speed and resultant wind speed is shown in the second panel of Fig. 11. The shading of the marks depends on the wind speed: the stronger the wind, the darker the marker. This is not an absolute scale. The meaning of the darkest color varies according to the values currently displayed. The data logger samples the instruments every 5 seconds (sampling rate = 5 s), including the anemometer. So, every 5 seconds we get a wind vector (with direction and magnitude). The data acquisition interval is 1 minute. This means that the CR10X collects wind vectors every 5 s for 1 minute. From these the data logger calculates the resulting vector. The so-called resultant wind direction and resultant wind speed is the direction and length of this vector, respectively. An illustration and more detailed description can be found in the CR10X data logger manual on page 11-2 (CR10X manual, 2022). The wind speed (blue dots on the second panel of Fig. 11) is the scalar sum of the length of the small wind vectors. If the wind directions variation is small or the wind speed is low, then the two wind speeds are close to each other. If the wind directions variation is high and/or the wind speed is also high, then the two wind speeds differ more.

Wind direction is shown at the bottom panel of Fig. 11. The shading of the marks depends on the wind speed in the same way as on the wind speed graphs. At the beginning of 31st August 2022, southerly winds blow. After sunrise, the wind started to be northerly. It is the effect of the Lake Fertő and it is called lake–land breeze circulation (Woodhams et al, 2022). This phenomenon is common at the observatory when the weather is not affected by fronts. After sunset, the water in Lake Fertő cools down more slowly than the coastal areas resulting in a temperature difference between the lake and the observatory. The warmer air rises above the lake and the air mass is replenished from the coastal areas. This means light southerly winds during nighttime. After sunrise, the coastal area warms up more rapidly than the lake, the air rises above the coastal area and northerly winds start to blow. On the examined day, the nighttime southerly winds did not return after sunset because of a cyclonic wave which had brought the precipitation in the afternoon.

Summary

This study describes the development of the main meteorological station at the NCK observatory between 2017 and 2022: from manual data acquisition to producing online plots which are updated quasi-real time every 10 minutes. In addition to describing the new data acquisition and processing system, the relocation of the meteorological measurements, for it to be closer to the atmospheric electricity measurements they support, was also discussed. Moving to a more open location also meant that measurements became less disturbed by the surrounding trees. We briefly described the two main instruments which were recently purchased: the LIDAR ceilometer and the visibility and present weather sensor. This was followed by a description of the plots on the observatory's website. A day with calm weather during the first half of the day was presented. On this day, the so-called lake–land breeze was observed, too. During the second half of the day, a precipitation system reached the station, so the LIDAR plots showed how cloud cover and precipitation appear in the data.

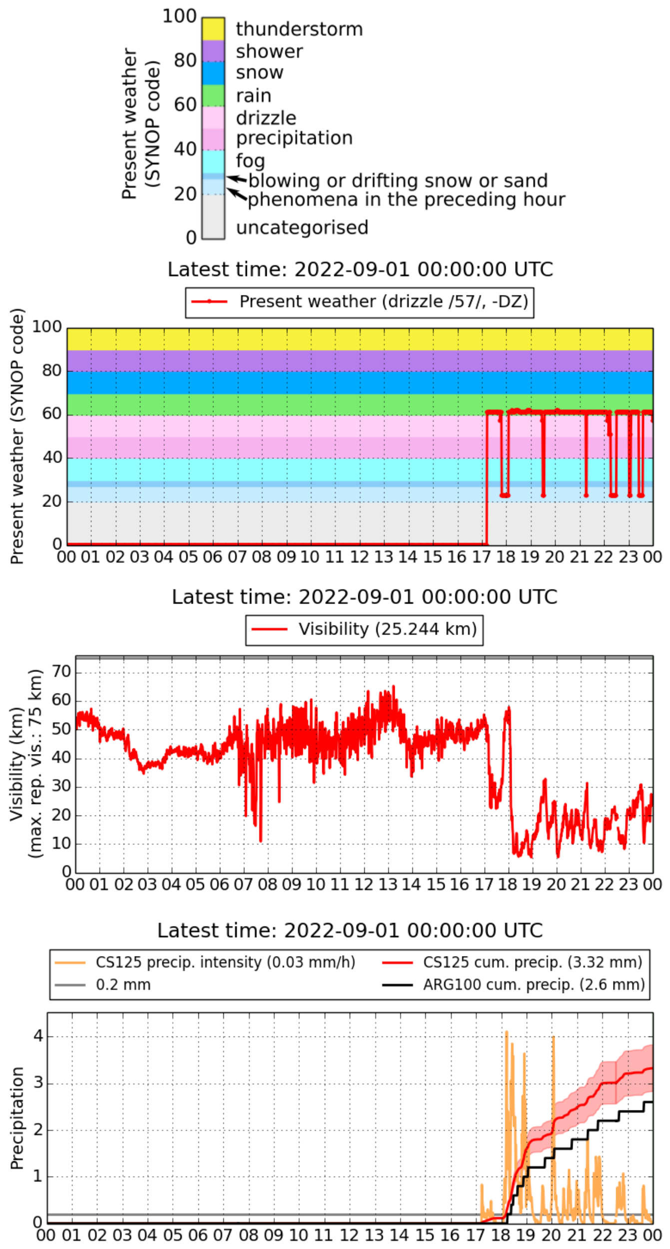

Fig. 9. Present weather (top), visibility (center), precipitation intensity (bottom, orange) and cumulated precipitation (bottom, red) obtained from the CS125 visibility and present weather sensor, and cumulated precipitation from the ARG100 tipping bucket rain gauge (bottom panel, black) at NCK on 31st August 2022.

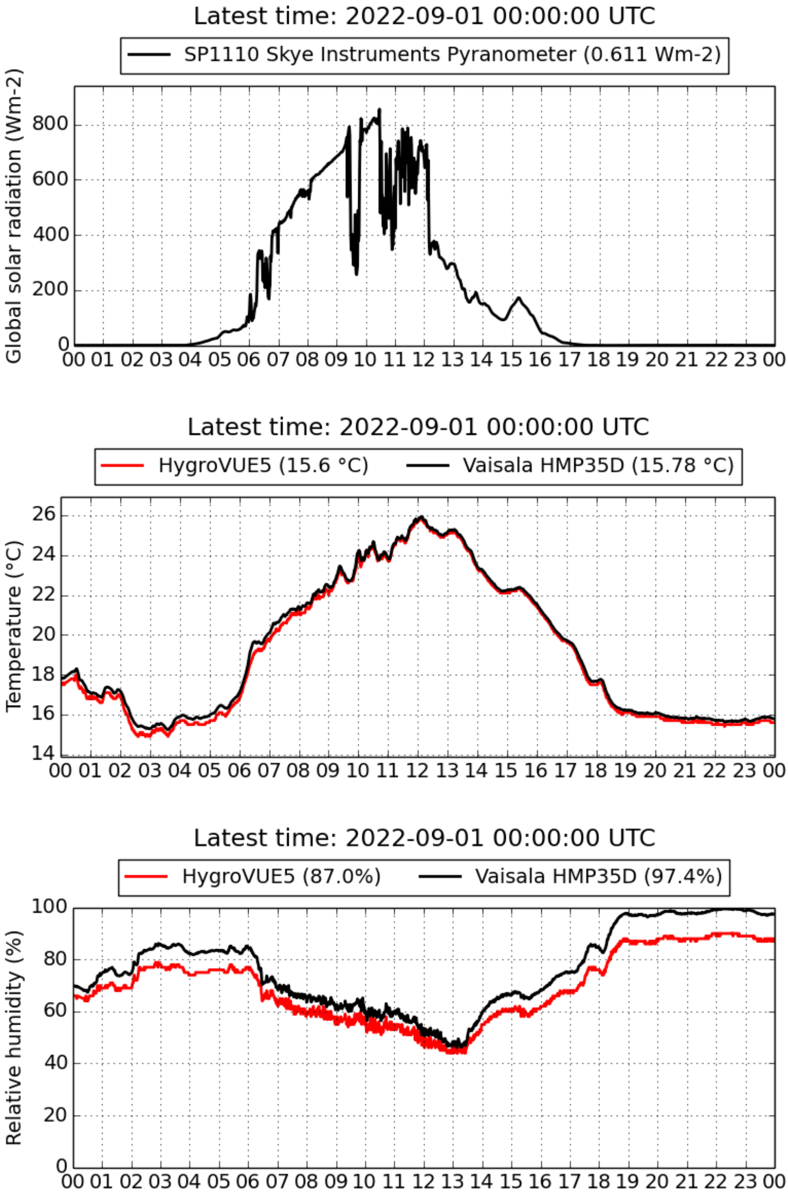

Fig. 10. Global solar radiation (top), temperature (center) and relative humidity (bottom) data at NCK on 31st August 2022.

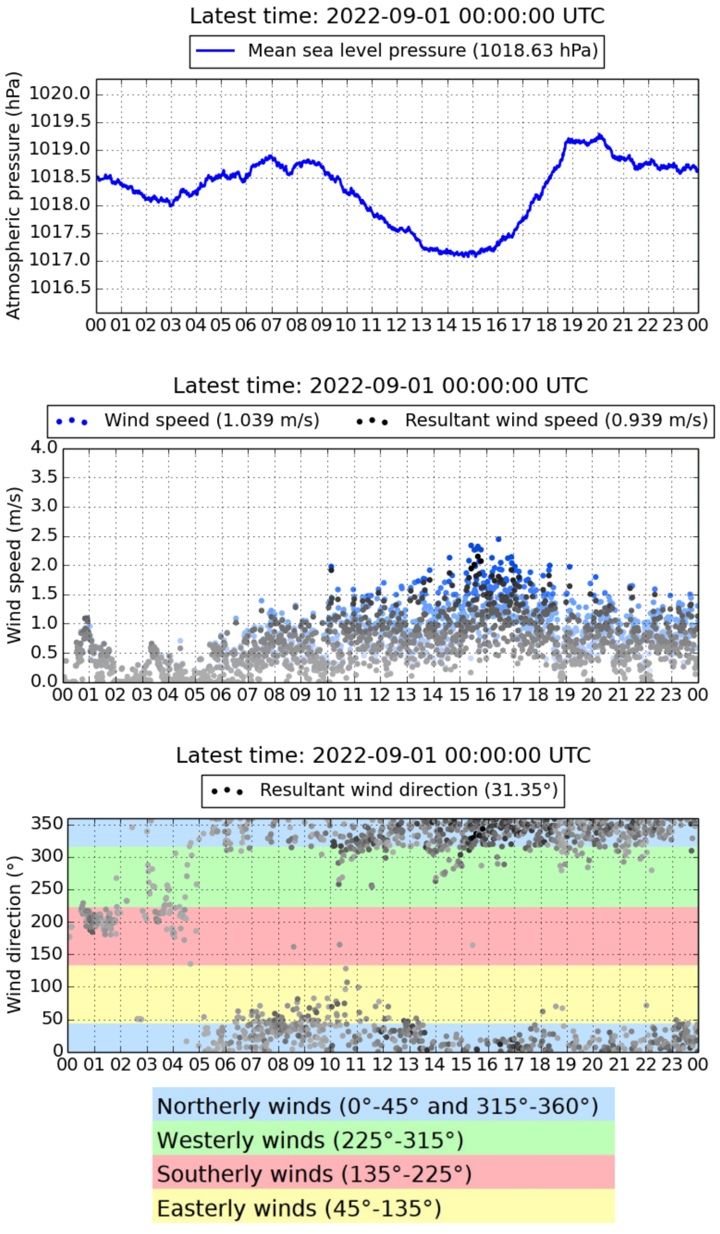

Fig. 11. Mean sea level pressure (top), wind speed (center) and wind direction (bottom) data at NCK on 31st August 2022.

Acknowledgements

This research has been supported by the National Research, Development and Innovation Office, Hungary (NKFIH; grant No. K138824) and the INFRA tender of the Eötvös Loránd Research Network (ELKH) in 2021. The authors would like to thank the collaboration opportunity and the assistance of the Hungarian Meteorological Services colleagues: Kornélia Radics, Gyula Horváth, István Sebők, Rita Hodossyné Rétfalvi and Hajnalka Baksáné Szini.

References

05103-LC (2022). Homepage of the Young Wind monitor (05103-LC). Available at: https://www.campbellsci.com/05103-lc. (Accessed: 21 October 2022).

ARG100 brochure (2022). Brochure of tipping bucket rain gauges. Available at: https://s.campbellsci.com/documents/ca/product-brochures/arg100-sbs500_br.pdf. (Accessed: 21 October 2022).

CR10X manual (2022). Manual of the CR10X data logger. Available at: https://s.campbellsci.com/documents/us/manuals/cr10x.pdf. (Accessed: 18 October 2022).

CS125 (2022). Homepage of the CS125 visibility and present weather sensor. Available at: https://www.campbellsci.com/cs125. (Accessed: 21 October 2022).

E-profile (2022). Available at: https://e-profile.eu/#/cm_profile. (Accessed: 18 October 2022).

EPSS news (2022). The technical handover of the Zero Magnetic Field Laboratory took place on 30 June 2022. https://epss.hu/en/magneses-nullter-laboratorium-muszaki-atadasa/ (Accessed: 21 October 2022).

Geophysical Observatory Reports, 1999–2001 (2003). Available at: https://gor.epss.hu/issues/GOR1999-2001/.

Harrison, R. G. and Nicoll, K. A. (2018). Fair weather criteria for atmospheric electricity measurements. *Journal of Atmospheric and Solar–Terrestrial Physics*, 179, 239–250. Available at: https://doi.org/10.1016/j.jastp.2018.07.008.

Hayden, B.P. and Pielke, R.A. (2022). Planetary boundary layer. *Encyclopedia Britannica*. Available at: https://www.britannica.com/science/planetary-boundary-layer. (Accessed: 21 November 2022).

HMP35D manual (2022). Manual of the Väisälä HMP35D humidity and temperature probe. Available at: https://s.campbellsci.com/documents/us/manuals/vaisala_hmp35a_manual.pdf. (Accessed: 21 October 2022).

HygroVUE5 manual (2022). Manual of the HygroVUE5 temperature and relative humidity sensor. Available at: https://s.campbellsci.com/documents/eu/manuals/hygrovue5%20-%201306.pdf. (Accessed: 21 October 2022).

Meteorological data at nckobs.hu (2022). Meteorological measurements at the Széchenyi István Geophysical Observatory website. Available at: https://nckobs.hu/data/met/. (Accessed: 18 October 2022).

Milrad, S. (2017). Synoptic Analysis and Forecasting: An Introductory Toolkit. *Elsevier*. Available at: https://doi.org/10.1016/C2015-0-05604-0.

PTB110 manual (2022). Manual of the CS106 Barometric Pressure Sensor (Väisälä PTB110). Available at: https://s.campbellsci.com/documents/us/manuals/cs106.pdf. (Accessed: 21 October 2022).

SkyVUE PRO manual (2022). Manual of the SkyVUE PRO ceilometer. Available at: https://s.campbellsci.com/documents/us/manuals/skyvuepro.pdf. (Accessed: 18 October 2022).

SP1110 (2022). Homepage of the Skye Instruments Pyranometer (SP1110). Available at: https://www.campbellsci.eu/sp1110. (Accessed: 21 October 2022).

Wikipedia (2022). METAR weather codes. Available at: https://en.wikipedia.org/wiki/METAR#METAR_weather_codes. (Accessed: 18 October 2022).

WMO (2019). WMO code table 4680: Present weather reported from an automatic weather station. In *Manual on codes: International Codes*, WMO Report No. 306, Geneva, Switzerland, A-360–A362. Available at: https://library.wmo.int/doc_num.php?explnum_id=10235#page=384.

Woodhams, B. J., Barrett, P. A., Marsham, J. H., Birch, C .E., Bain, C. L., Fletcher, J. K., Hartley, A. J., Webster, S. and Mangeni, S. (2022). Aircraft observations and sub-km modelling of the lakeland breeze circulation over Lake Victoria. *Quarterly Journal of the Royal Meteorological Society*, *148*(743), 557–580. Available at: https://doi.org/10.1002/qj.4155.